# Glass production at Jalame, Israel: Process, composition and relationship to Roman glass in Europe

Ian C. Freestone [a], Gry H. Barfod [b,*], Chen Chen [a], Katherine A. Larson [c], Yael Gorin-Rosen [d]

[a] UCL Institute of Archaeology, London WC1H 0PY, United Kingdom
[b] Department of Geoscience, Aarhus University, DK-8000 Aarhus C, Denmark
[c] Corning Museum of Glass, 1 Museum Way, Corning, NY 14830, USA
[d] Israel Antiquities Authority, POB 586, Jerusalem 91004, Israel

ABSTRACT

Following an initial micro-XRF assay, 42 samples of glass from the twentieth-century excavations of the fourth-century CE production site at Jalame, Israel, were selected and analysed by EPMA, with subsets for trace elements by LA-ICP-MS (n=29 samples) and for Hf isotopes by MC-ICP-MS (n=6). Comparison of major elements for ten samples originally measured in Brill (1988) was good, although the earlier $SiO_2$ values are slightly high. Analyses of furnace debris and contaminated glass imply that glass furnaces were made of, or lined with a lime-rich material, leading to contamination by CaO, rather than $Al_2O_3$. This confirms that higher alumina contents measured for Jalame glass relative to Roman Mn-decolourised glass of first-third century Europe are significant and it is suggested that the source of the earlier Roman glass lies further North on the eastern Mediterranean coast.

A wide range of trace elements are shown to have entered the glass with the addition of manganese, so caution should be exercised when interpreting trace element and isotopic data on glass with significant amounts of Mn, although the effects on REE and some of the lithophiles most often used in provenancing appear minor or insignificant in Jalame glass with MnO below 1.3 wt%. For example, the hafnium isotope composition of the Jalame material does not appear to have been significantly affected and falls within the previously determined Levantine range, distinguishable from Egyptian glass. Associated trace elements indicate that two Mn sources were exploited and this raises the possibility of further investigation of Mn sources in early glass production. The wide range of added manganese suggests problems in obtaining a homogeneous batch and it is suggested that (a) a single initially inhomogeneous furnace load melted to a range of colours, which were subsequently colour-sorted as chunks, and/or (b) the recycling of poorly fused manganese-decolourised glass into later manganese-free batches resulted in the observed variation.

The cobalt pigment used was the high-nickel late antique type and allows the introduction of this source to be pushed back from the sixth to the fourth century CE. The use of antimony in glassmaking ceased at around the same time, and it is speculated that these changes were related.

## 1. Introduction

The site of Jalame, northern Israel, was the location of one of the first excavations specifically undertaken to explore the production technology of Roman-period glass (Fig. 1). Directed by Gladys D. Weinberg and Paul N. Perrot, the excavations ran over several seasons from 1964 to 1971 and were a collaboration between the Corning Museum of Glass and the University of Missouri. The results remain an important point of reference for the study of glass of the fourth century CE, not least

because of the extensive analytical campaign undertaken by Robert H. Brill on the glass and its potential raw materials, which laid the foundation for our current understanding of natron glass production. In particular, Brill firmly identified the coastal sand of the area, along with Egyptian natron, as the raw materials, investigated the addition of manganese as a decolouriser (and identified its natural level in the raw batch at 0.03 wt%) and investigated colour generation in collaboration with J. W. H. Schreurs (Brill, 1988; Schreurs and Brill, 1984). Brill presented quantitative analyses of forty glass fragments, and this dataset

---

has been critical for attempts to classify Levantine glass on the basis of major elements (Freestone et al., 2000; Jackson, 2005; Phelps et al., 2016; Barfod et al., 2018, 2022a among others).

The dominance of the southeastern Mediterranean in the supply of primary glass from at least the fourth century BCE throughout the first millennium CE is well understood from a range of archaeological, philological and archaeometric evidence (Degryse, 2014; Gorin-Rosen, 2000, 2015; Rolland, 2021 among others). Dated to the mid-fourth century CE, primary glass production at Jalame can be expected to have played an important role in this trade, potentially representative of the Roman industry. Such an inference appears to increase the significance of the Jalame assemblage and its role as a reference dataset for Roman glass production. However, as the available data on Roman glassmaking has expanded, certain discrepancies have become apparent. As detailed below, rather than corresponding precisely to Roman glass vessels of the first-third centuries, the Jalame glass analyses show minor differences, in particular, reflected in a relatively high $Al_2O_3/SiO_2$ ratio (e.g. Henderson, 2002). The question of whether these differences are real has important implications with respect to the origin of Roman glass at the height of the Empire in the first-third centuries. Given the developments in analytical technique since the analysis of the Jalame assemblage in the 1970s (where, for example, $SiO_2$ was not measured directly but determined by difference), the possibility that the differences observed between Jalame and the more recently analysed Roman glass represent systematic analytical error is a real one and therefore requires testing. Furthermore, modern work is increasingly focused on the information from trace elements and isotopes which are largely lacking for Jalame.

The present paper revisits the scientific analysis of the glass finds from the Weinberg excavations at Jalame, incorporating a small selection of the glass previously analysed by Brill, along with a substantial group of previously unanalysed glasses. A major goal was to test if, in particular, the alumina and silica analyses from the 1970s-1980s can be reproduced by today's state-of-the-art techniques or if glass compositions at Jalame could be representative of 1st-3rd century Roman primary glass production. In view of the latter possibility, we also measured Hf isotopes for six samples from Jalame as well as for four Roman-Mn type samples recovered from London to confirm that these two types have identical values corresponding to production along the coast of the Levant. These will serve as reference data for future investigations. In addition, we present results on the investigation of ceramics and other debris from the site which have not previously been reported but which add to our understanding of the production technology and the relationship between the glass composition and the furnace material. Finally, we have taken advantage of the rare opportunity offered by the Jalame assemblage to investigate the addition of manganese to decolourise Roman glass and have constructed our sample selection to include a relatively wide range of manganese concentrations. The new dataset allows for investigation of the relationship between the raw materials, primary and secondary production waste to better understand the production methods including the use of manganese for decolourisation at the Jalame workshops.

## 2. The site and material

The site of Jalame, located southeast of Haifa in modern Israel, was excavated over four seasons from 1964 to 1971 by the University of Missouri and Corning Museum of Glass. It was occupied for several centuries in the Roman and Late Roman periods, with the Byzantine period occupation consisting of the remains of an extensive villa and



**Fig. 1.** (Left) Regional map of the Southern Levant showing glass production sites at Jalame, Apollonia, Bet She'an and Bet Eli'ezer as well as the cities of Akko, and Caesarea. (Right) Examples of the colours observed for the chunks analysed in this study.

olive and grape presses. The main focus of the excavations, however, was on the remains of a large glass workshop, dated to the second half of the fourth century CE (Fig. 1). While the overall phasing of the site has been re-interpreted (Slane and Magness, 2005), the original fourth century CE dating of the workshop remains valid.

The majority of waste from the glass workshop was found in a dump which covered an area of >150 square meters, located off the southwest edge of the hill. This waste included small glass chunks, moils and other glass-blowing debris, pieces of devitrified glassy material, and soft mudbricks. This debris clearly points to the secondary production stage, but the glass chunks, along with bricks and other building materials from the furnace also suggest a primary production stage, an interpretation supported by the recovery of partially reacted raw materials (Brill 1988: p. 284; see also below). It is unclear whether the dumping occurred during the life of the glass workshop, as a discard area for waste, or after the abandonment of the glass workshop, perhaps in preparation for the construction of a later Byzantine villa. The possibility of raw glass production at Jalame was not advocated in the original report (Weinberg, 1988), but a reappraisal by Gorin-Rosen (2015) identified the furnace structures excavated as a primary furnace for the production of raw glass. Recent excavations, close to those which provided the material analysed here, have furthermore revealed tank furnaces at Jalame of the typical form associated with primary glass production in the region (Gorin-Rosen, 2021; Sa'id and Gorin-Rosen, 2022). It is therefore clear that raw glass was made at Jalame; that the original excavations unearthed a primary glass furnace which was unrecognised as such at the time; and that the recovered assemblage includes partially reacted batch materials from the primary process. Hence, although the samples analysed here include the outputs of a secondary production process, all of the glass is likely to have been made from its raw materials at Jalame.

A total of 75 glass samples (18 chunks, 47 moils and 5 vessel sherds) were chosen from 40 boxes brought to Corning following the 1964–1971 excavations. The main criterion was to sample different classes of material (chunks, moils and vessels) exhibiting the entire range of observed colours including colourless, amber, bluish, bluish-greenish, greenish as well as the rare purple. We also wished to sample glass with a wide range of manganese contents. Furthermore, as each moil represents a blown vessel, our sample was biased towards moils as we were interested in the glass output of the site. Note therefore that the purple-coloured and colourless fragments are overrepresented relative to the general distribution of greenish-bluish hues in the assemblage (for the actual colour distribution for a large number of the moils, which had been consolidated into a single bag by Brill, see Fig. 2 and Larson, forthcoming). While there may be some unknown bias in this selection, as the criteria for Brill's sampling is unknown, Fig. 2 broadly confirms the general impression that the vast majority of glassworking at Jalame was of naturally coloured glass. Of the thousands of glassworking debris fragments stored in Corning, only a small handful were purple, colourless, or cobalt blue.

In addition, a number of fragments comprising floor, furnace ceramic, glass attached to ceramic or clearly contaminated glass were selected to represent the range of materials available and to understand the interaction between the glass and the furnace, and results on several informative samples are also presented.

## 3. Methods

Sample selection for analysis included ten (9 chunks, 1 moil) originally reported by Brill (1988) and five previously unanalysed vessel sherds, while 65 other samples were screened by $\mu$-XRF (micro-x-ray fluorescence; Table A1) and from this, a further 9 chunks and 18 moils were chosen. The final selection (42 samples in total) was chosen to ensure a full range of manganese contents (Table A2). The selected glass was sampled by chipping off fresh fragments measuring about 1 mm $\times$ 1 mm. These were mounted in epoxy and polished prior to analysis. Based on the EMPA and ICP-MS results (Table A2), we selected chunks with low (>0.06 wt%; Ch-2, Ch-5), intermediate ($\approx$ 0.2 wt%; Ch-10, Ch-11) and high MnO ($\geq$0.5 wt%; Ch-13, Ch-15) for Hf isotopic analysis (Table A3) to test the influence of Mn addition on the Hf isotopic composition of the bulk glass. For comparative purposes, four Roman-Mn type samples recovered from Basinghall Street, London (Freestone et al., 2015a), were analysed for Hf isotopes.

Several ceramic fragments (some with glass attached) were studied by thin-section petrography, while the glass–ceramic contact zones for selected samples were investigated using scanning electron microscopy (SEM-EDS).

### 3.1. $\mu$-X-ray

The chemical compositions of 44 moils were analysed by non-invasive $\mu$-X-ray fluorescence using a M4 Tornado Micro-XRF (Bruker Nano, Berlin, Germany). Exposed glass surfaces are likely to have experienced loss of, in particular, alkalis. Prior to analysis, a small area was therefore polished to remove the exposed layer using grinding foil coated with 15 um Silicon Carbide (SiC). Following polishing, the areas
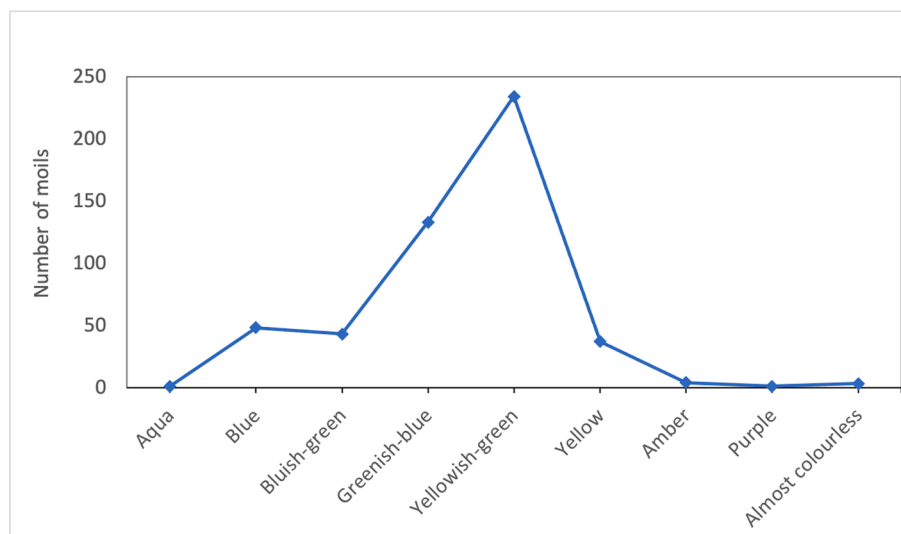


**Fig. 2.** Distribution of colours for a selection of 504 moils found at Jalame and kept at the Corning Museum of Glass.

were wiped with ethanol. The M4 Tornado with a rhodium (Rh) tube Rh target and a poly-capillary lens focuses the x-ray beam to a diameter of 20-$\mu$m at near-vacuum conditions (20 mbar). Settings during analysis included fluorescence radiation voltage of 50 kV and a current of 600 $\mu$A. Sample areas (typically 1 mm × 1 mm) were mapped with a dwell time of 10 ms/pixel. Results are reported in Table A1 as oxide weight percentages normalised to 100. Note that only elements with atomic number of 11 or above can be detected using this technique. Accuracy was estimated from repeated runs (n = 6) of Corning B glass standard from Corning Museum of Glass and was ~ 5 % for elements > 1 wt% (Table A1; Adlington, 2017). Exceptions include the $Al_2O_3$ and $Fe_2O_3$ concentrations that were 16 % too low and 8 % too high, respectively. The repeated runs of the Corning B standard further showed that concentrations below ~ 1 wt% for light elements such as MgO and $P_2O_5$ as well as below ~ 0.2 wt% for Cl and $TiO_2$ could not be determined precisely by the $\mu$-XRF screening, while PbO present at 0.6 wt% in the Corning B glass came out 20 % lower (Table A1). On the basis of this, we have selected not to report concentrations below 0.1 wt% for Cl, $TiO_2$ and PbO in Table A1. PbO concentrations in the samples all yielded values below 0.03 wt% with the exception of one vessel-sherd with 0.2 wt% (Table A1). For MnO, a high degree of correlation ($R^2$ = 0.98) between MnO concentrations obtained by $\mu$-XRF and EMP, showed a high accuracy down to 0.01 wt% by the $\mu$-XRF technique (Fig. A1).

### 3.2. EMPA

Major and minor elements were analysed by Electron Microprobe at Washington State University (WSU) on a JEOL JXA8500F with five wavelength dispersive spectrometers set at 20 kV acceleration voltage, 10 nA beam current and 10 $\mu$m beam. Calibration was done using NIST glasses, natural minerals and synthetic minerals. Repeated analyses of samples (n = 10) and Corning Museum Archaeological Glass Standard B (n = 10) showed reproducibilities in the order of 5 % for element concentrations above 1 wt% (Table A2; Brill, 1999; Adlington, 2017), while elements in low abundance (e.g. $Fe_2O_3$, MnO, $TiO_2$, $SO_3$ and Cl; Table A2; Vicenzi et al., 2002; Wagner et al., 2012) reproduced within about 15 %. Accuracies were 6 % relative or better for all elements except $TiO_2$, $SO_3$ and Cl with accuracies of 14%, 20% and 9%, respectively (Table A2).

### 3.3. LA-ICP-MS

Analysis by LA-ICP-MS was done at Washington State University on an Agilent 7700 spectrometer combined with a New Wave UP-213 laser, using line scans. Table A2 reports data as the mean of five repeats run at 12 J/$cm^2$ energy, 600 $\mu$m lines at 10 $\mu$m/sec, 60 $\mu$m spot size, 20 Hz pulse frequency and 70 sec data acquisition time with 10 sec blank. Data reduction in LADR software used NIST 610 standard glass as calibration and Si as internal standard. BCR-2 and Corning B were monitored for reproducibility and accuracy (Table A2). Generally, repeated analysis (n = 20) of BCR-2 throughout the two runs reproduced within 5% for most elements, whereas Li, B, Ti, Zn, As, Ag, Sb and Au had reproducibilities exceeding 10% (Table A2). Accurracies below 8 % were obtained for all elements except Li, B, Ti, Cu, Zn, As, Ag, Sn, La Tl that deviated by 10% or more from certified values (GeoReM; geochemical database for reference material and isotopic standards). Rare Earth Elements (REE) for BCR-2 reproduced within 2–4% and were within 0–7% of certified values. However, reproducibilities and accuracies of REE for the Jalame glass and Corning B standard are significantly worse due to the very low concentrations here compared to BCR-2 (<0.2 ppm versus 0.5 – 57 ppm; Table A2).

### 3.4. MC-ICP-MS

Aliquots of fresh glass weighing ≈0.05 g were dissolved in $HNO_3$-HF mixtures followed by several evaporation steps in 6 N HCl. The solutions

were loaded on columns loaded with AG50-X8 resin to remove iron followed by separation of Hf from REE etc. on Eichrom® Ln-spec using HCl-HF dilutions. The Hf isotopic compositions were measured at the UCDavis Interdisciplinary Center for Inductively-Coupled Plasma Mass Spectrometry on a Nu Plasma HR (Nu032). Mass fractionation correction was done by normalizing to the known natural ratio of $^{179}Hf/^{177}Hf$ of 0.732527. Every four to five samples, Ames Hf standard JMC-475 (n=10) was run and yielded a mean $^{176}Hf/^{177}Hf$ ratio of 0.282176 ± 0.000029 (2$\delta$) throughout the run, which matches the recommended value 0.28216 (Stevenson and Patchett, 1990; Vervoort and Blichert-Toft, 1999 among others); $^{176}Hf/^{177}Hf$ ratios for samples as well as Corning B and BHVO-2 were therefore not adjusted to this standard. USGS basalt standards BHVO-2 (n=1) yielded 0.283102 ± 0.000010 (2$\delta$) (compared to GeoReM recommended value = 0.283104 ± 0.000010), while glass standard Corning B (n=3) from Corning Museum of Glass yielded 0.282207 ± 0.000015 (2$\delta$), which compares well to 0.282212 ± 0.000015 (2$\delta$) previously measured (Table A3; Barfod et al., 2020, Barfod et al., 2022b). Monitoring $^{172}Yb$, $^{175}Lu$, $^{181}Ta$ and $^{182}W$ signals throughout the session showed signals were all less than a few mV. $\varepsilon_{Hf}$ was calculated from present-day CHUR values of 0.28278529 (Bouvier et al., 2008). Details on Hf separation and analytical methods are in Barfod et al. (2020).

### 3.5. Thin-section petrography

Four fragments of ceramic were prepared as petrographic thin sections. Because the samples are fairly friable, fragments were first mounted in epoxy resin blocks and then cut in two. One half was ground flat, mounted onto a glass microscope slide and ground down to 30 $\mu$m thickness with carborundum powder, while the other half was prepared for SEM-EDS analysis (see below). The thin sections were examined at magnifications of 50-200x in plane polarised light and between crossed-polars. The samples were characterised in terms of their inclusions, matrix and voids.

### 3.6. Scanning electron microscopy (SEM-EDS)

Composite glass–ceramic samples were ground using 600–4000 grit carborundum abrasive, polished with diamond pastes down to 1 $\mu$m, then vacuum-coated with carbon. The polished samples were examined using a ZEISS EVO 25 scanning electron microscope (SEM), fitted with an Oxford Instruments X-Max$^N$ 80 Silicon Drift Detector and Aztec Energy Dispersive X-ray Spectrometer (EDS) system. Working conditions were 20.0 kV accelerating voltage, 8.50 mm working distance, and 300 s counting time, with a typical yield of c. 3 million counts on metallic cobalt. Bulk analysis for glass samples was taken at 600x magnification for 1–5 different areas, and that for ceramics was typically at 250-300x magnification for 1–3 different areas. Oxygen was determined by stoichiometry and results were normalised to 100 wt%. The sessions were accompanied by EDS analyses of Corning Museum of Glass archaeological reference glasses (Brill, 1999; Adlington, 2017). For major oxides with a concentration>5%, relative errors (RE) were within 5% and relative standard deviations (RSD) within 2%. For most minor components (0.1–5%), relative errors were within 10% of the accepted values, but deteriorated as the detection limits of c. 0.1% were approached.

## 4. Results

### 4.1. Glass chunks, moils and vessels

#### 4.1.1. Major elements
Natron glasses are normally sub-divided on the basis of compositional features characteristic of the location and period of production (Freestone et al., 2000; Foy et al., 2003). Particularly useful discriminators relate to subtle differences of minor minerals in the glass-producing sands that are well illustrated by differences in the $Al_2O_3$/

SiO$_2$ and TiO$_2$/Al$_2$O$_3$ ratios for the natron glass types produced in Egypt and the Levant during the first millennium CE (Schibille et al., 2017; Freestone, 2021; Fig. 3). Based on the Al$_2$O$_3$/SiO$_2$ and TiO$_2$/Al$_2$O$_3$ ratios between 0.038 and 0.047 and below 0.035, respectively, the Jalame glasses in this study have similar ranges to glass of Byzantine (6-7th century) date produced at Apollonia on the Levantine coast (Fig. 3) and with the previous analyses from Jalame from Brill (1988; see below).

The complete major, minor and trace element dataset for the Jalame glass is reported in Table A2 and shows that most major elements are indistinguishable for the moils, chunks and vessels (e.g. Fig. 3); the only exceptions are MnO that ranges significantly for the chunks and moils (0.01 – 4 wt%; mean = 0.75), but shows a more restricted range and relatively high concentrations in the vessel sherds analysed here (0.75 – 2.5 wt%; mean = 1.3%; however, note that Brill (1988) reports vessels with lower Mn levels which are close to the sand background). In addition SO$_3$ concentrations in the vessel sherds (0.25 ± 0.07 wt%) are elevated relative to the chunks and moils (0.12 ± 0.06 wt%). Fe$_2$O$_3$ concentrations are similar for all groups except for vessel sherd Ve-2 with 1.1 wt% Fe$_2$O$_3$, which is more than double that observed for all other samples. As anticipated, the low MgO and K$_2$O values of all samples correspond to the use of natron (evaporitic soda sourced from Egypt).

MnO varies more-or-less continuously across the data set (Table A2, Fig. A2a). MnO contents of naturally-coloured glasses (translucent pale blues, yellows, greens, browns) vary from 0.01% − 0.97%; no systematic differences between the different tints could be recognised. MnO contents of colourless or near-colourless glasses range from 0.75% − 1.72%, while purple glasses have above 1.64% MnO. Overlaps around the thresholds between colours are minor and presumably this consistency is a reflection of the standardised sand and alkali raw materials and furnace conditions.

### 4.1.2. Trace elements

With the exception of two cobalt blue-coloured samples (Ch-14, Ve-2) with highly elevated Co, Cu, Ni, Zn, Ga, As, Mo, Ag, Sn, Sb, Tl and/or Pb, trace element concentrations are generally low and relatively homogeneous (Table A2) but show in some cases strong intercorrelations with Mn (Table A4). These include Mo, Co, W, Zn, Ba, V and Ni with R >

0.9 (see section 5.2 for more details). While Mo and Ba correlate strongly with Mn, they define two trends that appear to point towards two endmember manganese ores with different trace element signatures that we term Pyro1 and Pyro2 (Fig. 4).
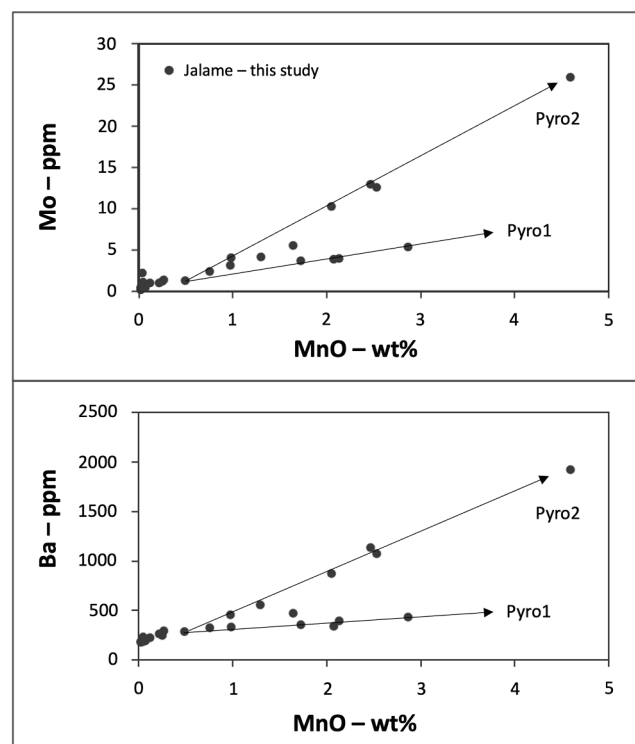


**Fig. 4.** Mo [ppm] and Ba [ppm] versus MnO [wt%] showing two distinct trends that appear to be controlled by two distinct endmembers, corresponding to ores with moderate and high Ba and Mo concentrations labelled Pyro1 and Pyro2, respectively.
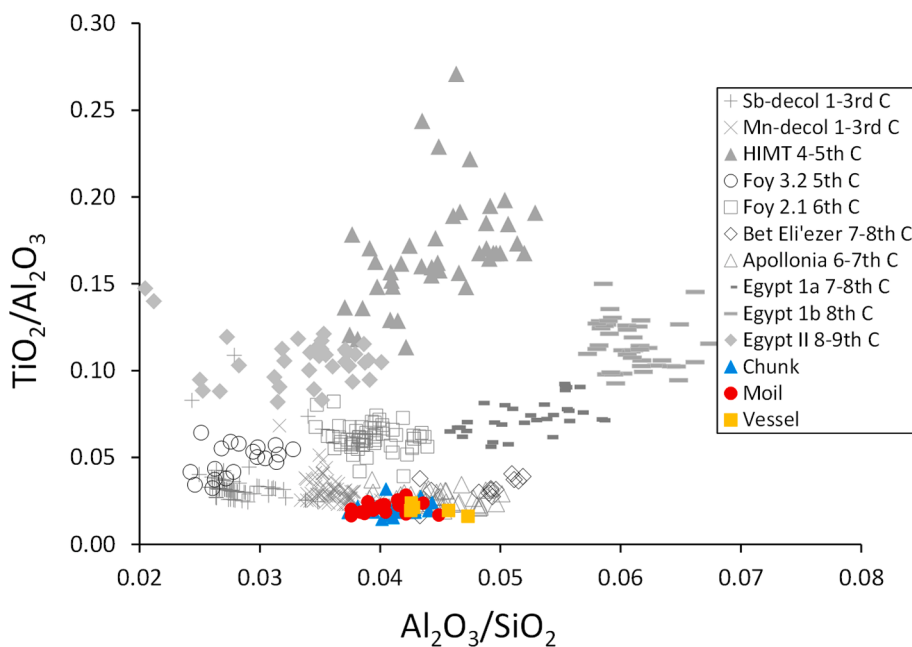


**Fig. 3.** TiO$_2$/Al$_2$O$_3$ versus Al$_2$O$_3$/SiO$_2$ for the glass from Jalame analysed in the present study (coloured symbols) compared with accepted categories of natron glass and our current best estimate of their production periods; in grey, data of Foy et al. (2003; HIMT, Foy 2.1, 3.2); Schibille et al. (2019; Egypt Ia, Ib, II), Phelps et al. (2016; Apollonia-type), Freestone et al. (2015b; Bet Eli'ezer-type), Silvestri (2008) and Silvestri et al. (2008; Sb- and Mn-decolorised).

### 4.1.3. Hf isotopes

The six chunks from Jalame analysed for Hf isotopes yield $\varepsilon_{Hf}$ values between −11.9 and −9.7 and, similarly, the four Roman-Mn glasses from London yielded $\varepsilon_{Hf}$ values between −12.2 and −11.3 (Fig. 5). $\varepsilon_{Hf}$ values above −12.2 correspond to previously analysed natron glass samples of typical Levantine elemental composition (Fig. 5; see also Fig. 3c in Barfod et al., 2020). For the Jalame glass, there was no observable change of isotopic compositions in samples with baseline MnO versus those with high MnO, showing that the addition of Mn did not significantly affect the $\varepsilon_{Hf}$ values of the glass.

### 4.2. Ceramics and contaminated material

Three mudbrick samples were found to consist of a highly calcareous marl (normalised compositions with > 60 wt% CaO, c.5 wt% $Al_2O_3$ and c. 20 wt% $SiO_2$) with very few quartz inclusions. Fossil foraminifera are visible, although the ceramic matrices are red and have lost birefringence so have been exposed to high temperatures (in excess of c. 700 °C), although not to the direct heat of the furnace interior.

A number of ceramics appear composite with pale or whitish areas. In the SEM, they are seen to comprise glass and high temperature Ca-rich minerals such as (in order of decreasing Ca/Si) larnite ($Ca_2SiO_4$), rankinite ($Ca_3Si_2O_7$), wollastonite ($CaSiO_3$) and combeite ($Na_2Ca_2Si_3O_9$). A gradation in some samples with Ca/Si ratio of the minerals increasing from glass to ceramic (e.g. Fig. 6) indicates that this is a reaction zone between the molten Na-Si-rich glass and Ca-rich furnace wall or lining such as marl brick, limestone or an applied lime layer. This is comparable to observations by Chen et al. (2021) for furnace wall – glass interactions in a Byzantine secondary production furnace at 'Aqir, Israel. A sample with a vitrified translucent white body with inclusions of wollastonite and devitrite ranging from tens to hundreds of micrometres probably formed by the more complete interaction of glass and Ca-rich ceramic at high temperatures. It is important to note that the inferred unreacted lime-rich furnace material was not found attached to these glassy samples; the reaction zone was bound to the glass and detached with it, separating from the more friable lime-rich furnace wall.

In contrast to the lime-rich interaction zones, white layers in several other samples are composed mainly of relict quartz and a dendritic silica polymorph (tridymite or cristobalite) (Fig. 7). The quartz particles are well-sorted, mostly < 200 μm in size. Although edges are poorly defined



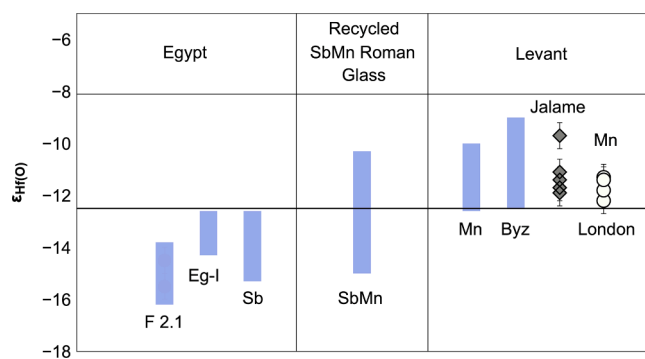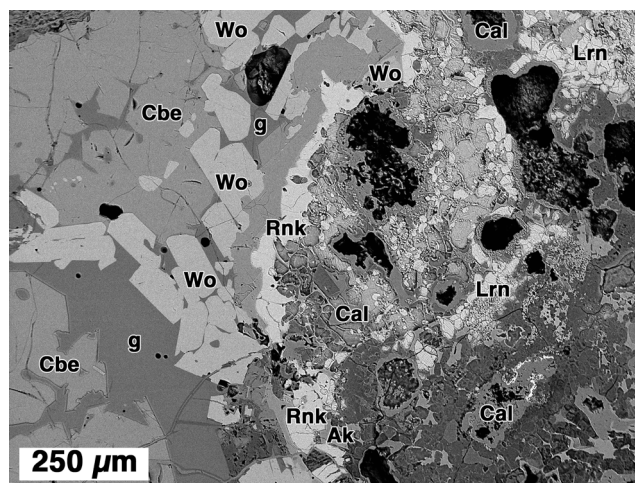**Fig. 6.** Back-scattered electron image of sample 455–2; a reaction zone between glass and Ca-rich ceramic. Cbe = combeite, g = glass (composition see 455–2-Al), Ak = alumoåkermanite, Wo = wollastonite, Rnk = rankinite, Lrn = larnite, Cal = calcite. Note the general increase in Ca/Si of the mineral phases moving left to right in the micrograph. Calcite is seen to line pores and its distribution is thus considered to reflect post-depositional processes.
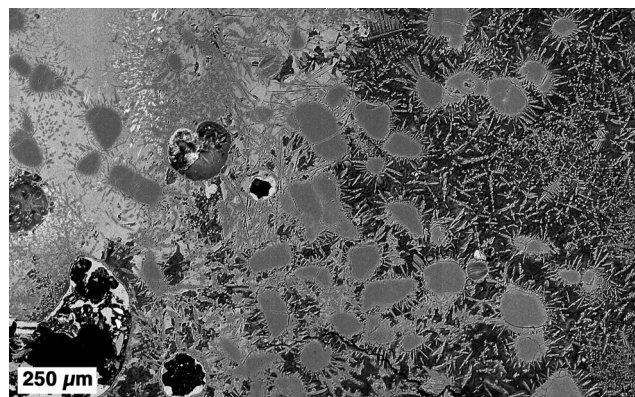


**Fig. 7.** Back-scattered electron image of sample 816–2 with light grey glassy area top left. The tiny white particles are wollastonite. The grey particles are relict quartz sand with dendritic silica rims. The white deposit in the large pore (bottom left) is Cu-Sn rich, and may reflect secondary deposition due to burial close to an artefact of copper alloy (see Oikonomou et al. (2023) for similar features in primary glass production elsewhere). To the right of the figure, the silica-depleted glass around the dendritic phase has corroded, leaving a low atomic number (dark) hydrated residue.

due to the precipitation of the silica polymorph, these quartz particles are similar in size and shape to a sample of sand from the mouth of Belus River in modern Haifa Bay (kindly provided for comparison by Ms. Lisa Pilosi of the Metropolitan Museum, New York). This location was famous for high-quality glass-making sands in the Roman period. Therefore, chunks of this type are probably primary glass with relict glass-making sand and strongly suggest the presence of primary glass-making on the site, which is consistent with its re-assessment as a primary production centre, which also included a secondary workshop operating in the same area.

## 5. Discussion

### 5.1. Comparison to Brill (1988)

Table A5 compares the EMP results obtained in this study for ten samples which were previously reported by Brill (1988) by atomic absorption spectrometry (AAS) and semi-quantitative optical emission



**Fig. 5.** Hf isotopic compositions for Jalame and other natron glass types in the first millennium CE showing the difference in $\varepsilon_{Hf}$ values observed for Egyptian (<-12.2) versus Levantine (>-12.2) glass. From the Levant (right panel from right): Mn London (Mn Roman glass from London; this study); Jalame (this study); Byz (Jalame-like and Apollonia-like glass recovered from Jerash, NW Jordan) and Mn (Mn Roman type glass recovered from Jerash). From Egypt (left panel): Foy 2.1, Egypt-1 and Sb Roman type glass recovered from Jerash, N Jordan. Range for SbMn Roman glasses (middle panel) includes compositions observed for recycled Roman glass from Jerash and Ribe, Denmark. Comparative data from Barfod et al., 2020, 2022b. Uncertainties (2σ = ± 0.4 ε units), estimated from repeat analysis of the JMC-475 Hf standard, are displayed as error bars on individual $\varepsilon_{Hf}$ analyses.

spectrography (OES). This shows values for the same samples that are within a few percent relative for $Al_2O_3$ and for most other elements present in amounts above 1 wt%. Only in the cases of very low concentrations ($TiO_2$ and MnO < 0.1 wt%) do the duplicates deviate substantially, by up to 90 %. This is likely to reflect well-known limitations of OES, but possibly also inhomogeneous distribution of MnO in the glass. Fig. 8, comparing alumina versus silica for the complete datasets, suggests the possibility of a slight bias towards higher $SiO_2$ for the data reported by Brill, which may reflect the determination of $SiO_2$ by difference in his study (Brill, 1999 vol 2, p. 6 acknowledges that silica values are "a little high"). Overall, however, the major and minor element concentrations obtained by Brill (1988) reproduce extremely well. There is something of a "tail" for the new data on the low-silica (left hand side) of Fig. 8, which includes a number of glasses with high manganese contents. This "tail" is a simple dilution effect and disappears when the samples are plotted as reduced compositions without MnO, causing the Jalame data to form a much tighter cluster ranging from 67 to 73% $SiO_2$* (Fig. A2b).

The overlap between Brill's and our new dataset not only confirms that chemical differences exist for Jalame versus earlier Roman Levantine glass, but also that the chemistry of Jalame glass may be distinguished from the later Byzantine-Islamic productions at Apollonia (6-7th century) and Bet Eli'ezer (8th century). A plot of $CaO/Al_2O_3$ versus $Na_2O/SiO_2$, which has been previously used to distinguish these productions (Al-Bashaireh et al., 2016; Phelps et al., 2016) confirms that the key difference is in the $Na_2O$ content, reflecting the decrease in the quantity of natron added to Levantine glass over time (Freestone, 2021). Note, however, that this ratio plot (Fig. 9) obscures the differences between fourth century Jalame and earlier Roman-Mn, which are apparent in the $Al_2O_3/SiO_2$ ratio (Figs. 3 and 8).

### 5.2. Roman versus Jalame glass

Figs. 3 and 8 emphasise a significant difference between Jalame and earlier Roman productions. Roman glass from the 2nd-3rd centuries is characterised by lower alumina than the Jalame glass, which has $Al_2O_3$ levels similar to later Byzantine glass from Apollonia, further to the South. While alumina is generally considered to be a potential contaminant from the melting pot or furnace, and this has been demonstrated to be so in some cases (Jackson and Paynter, 2016), it is shown above that the contact zones between the furnace walls and the

glass are rich in lime and low in alumina. The relatively high $Al_2O_3$ in the Jalame glass is thus unlikely to represent contamination. Rather this compositional distinction is likely to represent true differences in the sand used to produce the earlier Roman and Jalame glasses. Analyses of glass from Levantine workshops south of Haifa (and thus south of Jalame) have consistently yielded compositions which are high in alumina (around 3 wt% $Al_2O_3$); significantly higher than Mn-decolourised glass of the first-fourth centuries (Chen et al., 2021; Freestone et al., 2000, 2008, 2015b; Jackson, 2005; Jackson and Paynter, 2016; Tal et al., 2004, 2008). This may be explained by the transport of the sand along the eastern Mediterranean coast.

Alumina in the coastal sands of the Levant is mainly controlled by the Nile tributaries that, in addition to the predominant quartz, carry Al-rich minerals (such as amphibole, plagioclase and clays) to the mouth of the Nile delta from where they are transported by longshore drift northeastwards along the Levantine coastline. Progressively lower concentrations of these Al-bearing minerals from the Nile delta to the Bay of Haifa have been shown to reflect partial loss of these minerals during transport (Emery and Neev, 1960; Stanley, 1989; Be'eri-Shlevin et al., 2014). Lower concentrations of alumina are therefore to be expected in the sands to the North of Apollonia and Jalame. Although there are likely to have been complicating factors in this effect over geological time, it is therefore tempting to suggest that the earlier, lower alumina Roman glass production of the first to third centuries was to the North, around Mount Carmel itself or possibly at Sidon, which was known as a glassmaking centre in antiquity (Trowbridge, 1930), and/or at Beirut, where primary glassmaking furnaces have been reported by Kouwatli et al. (2008). It is interesting to observe that, at the present time, analysed primary glassmaking installations uncovered from Israel are of Late Roman to Islamic date, while primary glassmaking remains have not yet been published from earlier periods in the region.

The difference in composition between glass produced at Jalame and earlier Roman glass does not necessarily mean that raw glass from Jalame was not widely distributed; "Levantine I" glass from fourth-century CE contexts in Italy (Maltoni et al., 2016) and Britain (Foster and Jackson, 2009) appears to correspond to the Jalame type and is likely to have originated here.

However, Levantine glass is frequently subordinate to Egyptian HIMT glass which appears to have been more extensively used in the West (Foster and Jackson, 2009; de Juan Ares et al., 2019).

### 5.3. Manganese and trace elements

Manganese was added to the Jalame glass as both a decolouriser (oxidizing bluish ferrous oxide in the batch to pale yellow ferric oxide) and, at concentrations above about 1.7 wt%, as a colourant (Fig. A2a; Brill, 1988; Schreurs and Brill, 1984). As noted by Gliozzo (2017) most authors assume that the additive was naturally-occurring pyrolusite ($MnO_2$). The strong oxidative power and its common occurrence make pyrolusite a far more likely source than rarer and more reduced manganese oxides such as hausmannite ($Mn_3O_4$); however, the use of hydrated forms of manganese oxide, typically described under the umbrella terms "psilomelane" or "wad" is possible. Indeed, Egyptian manganese ores (potential sources for the Mn in Levantine glass) appear to typically comprise pyrolusite along with hydrated Mn-minerals (although the supporting evidence for these identifications is often unclear; c.f. Kora et al., 1994; Sedki et al., 2019).

The confirmation of Jalame as a raw glass making centre implies that most, perhaps all, of the recovered glass from the site was made there from its raw materials. This is fully consistent with the relatively narrow compositional distribution of the new analytical data (when MnO is excluded; see above, Fig. A2b). It would also imply that manganese was added to the glass at the primary stage, as many of the chunks contain concentrations of Mn above the background level of 100–200 ppm, an estimate based upon the lowest values obtained in the present LA-ICP-MS dataset. Such low Mn contents in the glassmaking sands are
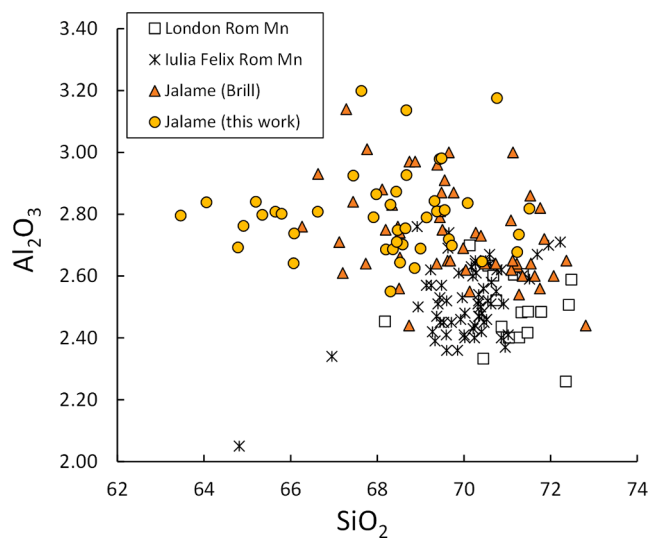


**Fig. 8.** Alumina [wt%] versus silica [wt%] for Jalame glass as analysed here and by Brill (1988) compared with 2nd-3rd century Mn-decolourised glass from London (Freestone, previously unpublished EPMA; Table A6) and from the Iulia Felix wreck (Silvestri, 2008, Silvestri et al., 2008).
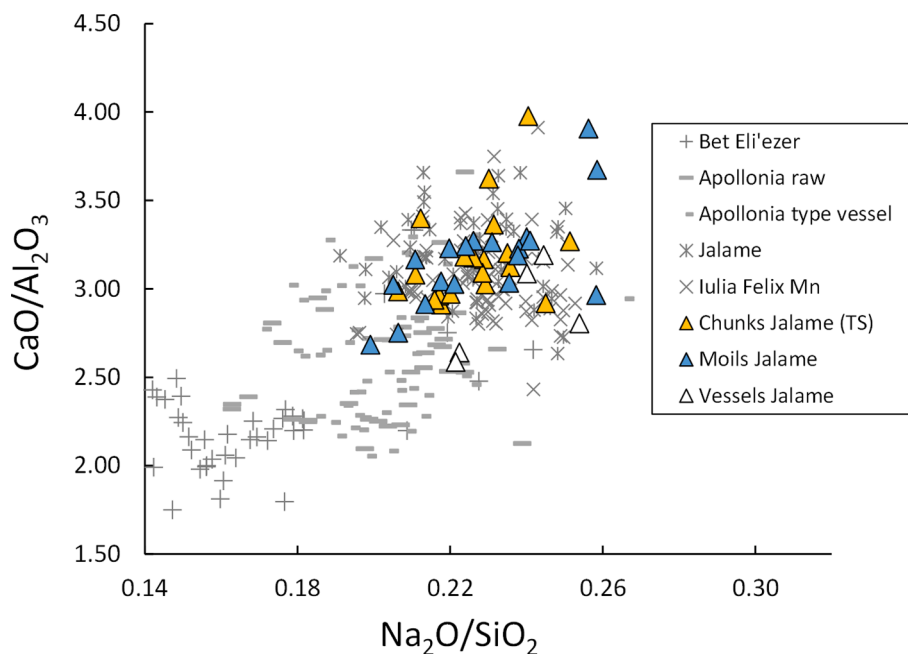
**Fig. 9.** $CaO/Al_2O_3$ versus $Na_2O/SiO_2$ showing the overlap between data from Brill (labelled Jalame) and this study (triangles). This confirms the overall decrease in $CaO/Al_2O_3$ and $Na_2O/SiO_2$ ratios (and thus in the proportion of natron relative to quartz) in the glass groups over time (Jalame 4th century, Apollonia 6-7th century and Bet Eli'ezer 8th century).

confirmed by the similar levels in glass from the primary furnaces at Apollonia and Bet Eli'ezer where manganese was not added as a decolouriser or colourant (Brems et al., 2018). This estimate of baseline manganese content is also in line with those made elsewhere, including by Brill (1988) and Schibille et al. (2017). The dataset in the present study therefore offers an important resource to examine the production of Mn-decolourised glass, and the effects of manganese on glass composition. In the following discussion, three samples with colourant levels of cobalt or copper, which contain a range of trace transition metals added with the colourant, are excluded (Ch-6, Ch-14 and Ve-2; highlighted with blue in Table A2). This leaves twenty-seven samples analysed by LA-ICP-MS, with MnO ranging from below 0.03 to 4.6 wt% (Tables 1 and A2; Fig. 4) that we feel confident were made using sand from the same source. The manganese ore is likely to have contributed a range of other elements to the glass, not only from the assumed pyrolusite or manganese oxyhydroxide phases, but also from minor minerals which are likely to have been present (e.g. Araffa et al., 2020).

To investigate the effect of the manganese additions, the dataset was divided into groups based upon manganese content, shown in Table 1. For the groupings, cut-off values were chosen where there were interruptions in the relatively smooth and continuous distribution of MnO concentrations (Fig. A2a); however, they could be the result of our limited sample size. The samples with the highest MnO (>1.3%) fall into two distinct manganese groups, Pyro1 and Pyro2 (see above; Fig. 4). This results in six groups in all (Table 1): glass with MnO equivalent to the sand background (<0.03 wt%), low-Mn (0.03–0.08 wt%), med-Mn (0.1–0.5 wt%), high-Mn (0.7–1.2 wt%), Pyro1 (>1.3 wt%) and Pyro2 (>1.3 wt%). Mean elemental compositions for the subgroups were normalised to mean concentrations observed for the background group and are compared in Fig. 10a-c. Here, it is clear that a significant range of trace elements are enriched in the glass when Mn is added. These can be divided into two groups: those elements highly enriched in and strongly correlated with Mn (R > 0.9; Mo to Ni in Fig. 10c) and exemplified by W versus MnO (Fig. 10a) and those elements that are less enriched and typically show a weaker correlation, but which still appear elevated in the glasses with MnO above 1.3 wt% (Y to As in Fig. 10c; exemplified by Sr versus MnO; Fig. 10b). It seems likely that the mineralogy of the Mn-source plays a part in these complex relationships.

The group of elements strongly correlated with MnO are those which tend to occur in manganese-bearing minerals (Mo, Co, W, Zn, Ba, V, Ni), while the less strongly correlated but still enriched elements (Y, Sr, Zr, REE, Hf, Ga, As) represent minerals present as gangue in the manganese ores, but which are not themselves rich in manganese, such as zircon and REE-bearing phases.

For the less strongly correlated group, the effects of small additions of the elements can be masked by various correlations which occur in the sand itself, and this is exemplified by the relationship between Sr and Nd. Fig. 11a shows a marked overall strong correlation between Sr and Nd in the Jalame glasses. However, on this figure, MnO concentrations shown next to datapoints for low-Mn and Pyro2 group samples indicate a control from Mn on the Sr-Nd correlation at MnO values above 1.3 wt % (exemplified by Pyro 2 samples). In contrast, the Mn concentrations in the low-Mn group samples vary independently of Sr and Nd concentrations and thus appear to have no control on the observed correlation between these two latter elements (Fig. 11a). For instance, within the Low Mn group, the sample with the lowest Sr and Nd has the highest Mn concentration (0.07 wt% Mn; Fig. 11a). Thus, the strong correlation for Sr-Nd at *low* MnO concentrations (0.03–1.3 wt%) is independent of Mn.

When comparing Sr and Nd data for Jalame samples with MnO below 1.3 wt% with those from a single tank furnace at Apollonia (Fig. 11b; Brems et al., 2018), it is observed that a similar correlation appears to be present in the Apollonia glass where no manganese was added (meaning that MnO levels here are at background and originating from the glassmaking sand). Therefore, for the Sr and Nd correlation at Jalame two distinct effects may be seen: (1) a correlation which is characteristic of Levantine glassmaking sand and (2) a correlation resulting from the addition of large quantities of manganese. The first effect is independent from MnO addition (as also illustrated by the observations from Apollonia). The mineralogical origins of the Sr-Nd correlations in the sands are not yet clear and require detailed elemental as well as isotopic analysis. Note that similar correlations between Nd and Sr were observed by Oikonomou et al. (2018 in their Fig. 4) for natron glass of Hellenistic date.

These results have important implications for the understanding of raw materials and provenance studies of glass and show that the addition of $MnO_2$ as a decolouriser or colourant can significantly disturb

**Table 1**
Mean concentrations of major and selected trace elements by EMPA and LA-ICP-MS for groups of Jalame glass divided on the basis of Mn content. Full data in Table A2.

| | $SiO_2$ | $Al_2O_3$ | $Fe_2O_3$ | MnO | MgO | CaO | $Na_2O$ | $K_2O$ | $P_2O_5$ | Ti | V | Mn | Co | Ni | Zn | Sr | Mo | Ba | W |
|---|---|---|---|---|---|---|---|---|---|---|---|---|---|---|---|---|---|---|---|
| **Background Mn (n=5)** | | | | | | | | | | | | | | | | | | | |
| <0.03 wt% MnO | 70.3 | 2.86 | 0.26 | 0.02 | 0.44 | 8.12 | 15.4 | 0.76 | 0.06 | 275 | 6.79 | 120 | 1.02 | 3.25 | 7.41 | 354 | 0.30 | 184 | 0.07 |
| Std dev | 1.3 | 0.22 | 0.03 | 0.00 | 0.09 | 0.44 | 1.4 | 0.08 | 0.01 | 24 | 1.43 | 4 | 0.15 | 0.41 | 0.38 | 2 | 0.24 | 3 | 0.00 |
| **Low Mn (n=6)** | | | | | | | | | | | | | | | | | | | |
| 0.03–0.08 wt% MnO | 69.2 | 2.78 | 0.35 | 0.06 | 0.55 | 8.85 | 15.6 | 0.72 | 0.08 | 349 | 8.79 | 388 | 1.44 | 3.95 | 11.8 | 403 | 0.97 | 201 | 0.09 |
| Std dev | 1.2 | 0.09 | 0.08 | 0.02 | 0.15 | 0.66 | 0.7 | 0.13 | 0.01 | 91 | 1.49 | 141 | 0.12 | 0.44 | 1.4 | 59 | 0.67 | 18 | 0.02 |
| **Med Mn (n=6)** | | | | | | | | | | | | | | | | | | | |
| 0.1–0.5 wt% MnO | 68.4 | 2.76 | 0.33 | 0.28 | 0.48 | 9.09 | 15.7 | 0.79 | 0.09 | 338 | 9.01 | 2099 | 2.47 | 4.21 | 13.9 | 423 | 1.15 | 264 | 0.11 |
| Std dev | 1.5 | 0.11 | 0.06 | 0.12 | 0.06 | 0.80 | 0.7 | 0.09 | 0.02 | 17 | 0.62 | 1177 | 0.22 | 0.25 | 2.2 | 48 | 0.17 | 27 | 0.02 |
| **High Mn (n=3)** | | | | | | | | | | | | | | | | | | | |
| 0.7–1.2 wt% MnO | 68.0 | 2.91 | 0.40 | 0.93 | 0.62 | 8.55 | 15.5 | 0.65 | 0.09 | 407 | 13.1 | 7174 | 3.93 | 6.77 | 20.2 | 498 | 3.18 | 370 | 0.15 |
| Std dev | 1.7 | 0.16 | 0.03 | 0.12 | 0.08 | 0.19 | 0.4 | 0.08 | 0.02 | 21 | 1.0 | 1647 | 0.74 | 0.97 | 6.0 | 18 | 0.86 | 73 | 0.02 |
| **Pyro1 (n=4)** | | | | | | | | | | | | | | | | | | | |
| >1.3 wt% MnO | 66.4 | 2.73 | 0.39 | 2.20 | 0.44 | 9.25 | 15.4 | 0.83 | 0.10 | 384 | 18.1 | 15,995 | 6.99 | 11.7 | 27.1 | 503 | 4.21 | 381 | 0.35 |
| Std dev | 2.4 | 0.07 | 0.06 | 0.48 | 0.02 | 1.36 | 0.1 | 0.11 | 0.02 | 101 | 5.6 | 3493 | 1.13 | 1.9 | 8.8 | 29 | 0.77 | 42 | 0.07 |
| **Pyro2 (n=6)** | | | | | | | | | | | | | | | | | | | |
| >1.3 wt% MnO | 66.2 | 2.80 | 0.45 | 1.99 | 0.55 | 8.69 | 15.9 | 0.77 | 0.11 | 402 | 21.1 | 14,674 | 9.46 | 8.86 | 30.9 | 525 | 9.08 | 823 | 0.24 |
| Std dev | 1.3 | 0.02 | 0.06 | 0.53 | 0.06 | 0.52 | 0.6 | 0.07 | 0.01 | 36 | 4.6 | 3752 | 2.07 | 1.00 | 9.7 | 25 | 4.05 | 298 | 0.04 |

some trace element concentrations in the glass. It affects not only the anticipated transition metals (elevated by factors of 4 or more by manganese additions of around 2.5%; Mo-Ni in Fig. 10c), but also the less expected lithophile elements such as the lanthanide rare earths, Zr, Hf and Y, which are commonly used in provenance investigations and may be modified by a factor of around 1.2 (see discussion above; Y-As in Fig. 10c, 11a). First and foremost, the concentrations of contaminating elements in the Mn ore depend upon its mineralogy and hence its source. For example, it has been demonstrated here that two types of manganese ore, designated Pyro1 and Pyro2, were exploited at Jalame, while two other distinctive types appear to have been used in the production of HIMT glass in Egypt (Freestone et al. 2018). While it appears that additions of MnO below 0.1 wt% have a minimal effect on the concentrations of the lithophile elements, concentrations above 1.3 wt% appear to be significant. On the basis of our data, we would therefore advise caution when comparing the sand-related components of glasses containing >0.5 wt% added MnO.

We also note that added manganese may potentially affect the isotopic composition of the glass, as has been previously observed for $^{87}Sr/^{86}Sr$ (Ganio et al., 2012; Gallo et al., 2015). For the main sand-related Nd isotopic system we observe an addition of Nd for samples with MnO above 1.3 wt% (Pyro1-2 groups) as previously inferred for HIMT glass (Freestone et al., 2018). While we do not have data for Nd isotopes in the glass from Jalame, the previous studies did not indicate a significant effect (Ganio op. cit.). There is a possible slight increase in Hf with Mn but it does not appear to have affected the measured Hf isotopic values for the Jalame samples; samples Ch-8 with 838 ppm Mn and Ch-15b with 13,599 ppm Mn both have $\varepsilon_{Hf}$ of 11.1 (see section 4.1; Table A3). Finally, there may be an increase in Pb with MnO, although the scatter of the data means that the magnitude of this cannot be confirmed.

### 5.4. Decolourisation practices

It is suggested above that the low concentrations of MnO in much of the Jalame glass imply addition at the primary stage and there is a strong case that the majority of manganese additions to glass in antiquity and the early medieval period were made at the primary rather than secondary stage of production: (1) the presence of manganese-containing natron glass at the primary production sites of the Wadi Natrun (see Nenna et al., 2005); (2) manganese in (plant ash) glass from the primary tank furnaces at Tyre (Freestone, 2002) as well as at Bet She'arim (Brill and Wosinski, 1965); (3) manganese in HIMT raw glass, (e.g. at Carthage, Freestone et al., 2018) and in chunks of raw glass from shipwrecks off the coasts of Israel and Sicily (authors' own work). Finally it is noted that there is very clear evidence that antimony decolouriser was added to Egyptian glass at the primary stage (Nenna et al. op. cit.), so by analogy it would seem likely that Mn was added at this stage in the Levant. Even so, it must be acknowledged that the Jalame assemblage is a mixture of the products of primary glassmaking (raw glass chunks) and secondary fabrication (moils, vessels, potentially glass chunks broken out of a secondary furnace) and the stages at which decolourisation and colouration took place must therefore be inferred.

The distribution of the Jalame base glass compositions, along with the evidence for both primary and secondary production at the site, strongly suggests that all of the glass analysed is likely to have been made there from raw materials. However, the wide range of added MnO contents raises a number of issues about production practice. It is generally considered that a significant excess of MnO over $Fe_2O_3$ was required to fully decolourise glass or to produce purple (e.g. Bidegaray et al., 2019; Silvestri et al., 2005; Zoleo et al., 2015). The Jalame glass typically contains 0.3–0.4 wt% $Fe_2O_3$ and, for both the new dataset and Brill's data, purple glass typically has in excess of 2 wt% MnO, while colourless glass has up to 1.7 wt% MnO (Table A2, Fig. A2a).

Much of the Jalame glass, typically tinted weak blue or green (Fig. 1), has MnO above the natural baseline derived from sand but
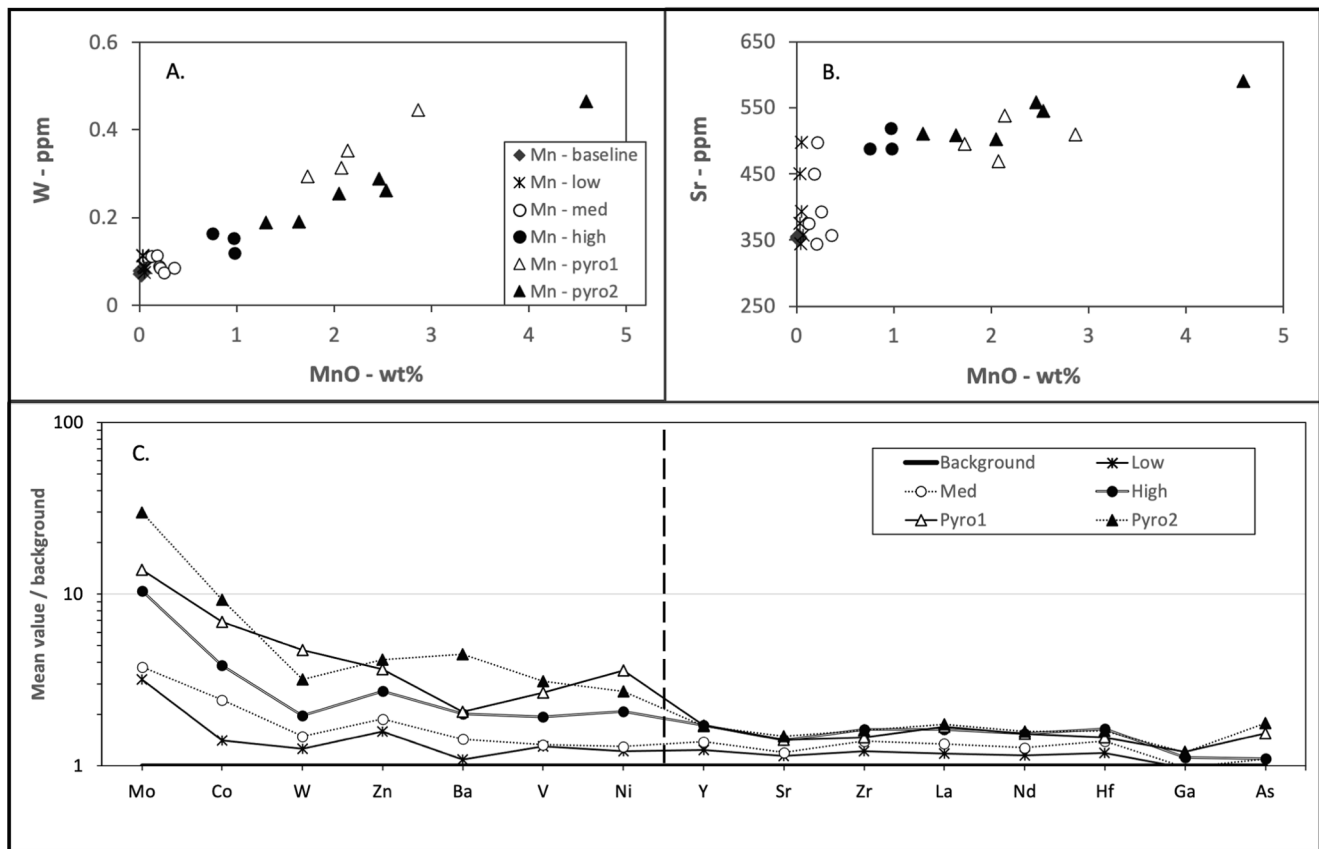
**Fig. 10.** (A). Example of an element (W) that correlates strongly with MnO and (B) an element (Sr) that shows an increase in samples with Mn above 1.3 wt%. c. Diagram showing mean values for trace elements in low (0.03–0.08 wt%), med (0.1–0.5 wt%), high (0.7–1.2 wt%), Pyro1 (>1.3 wt%) and Pyro2 (>1.3 wt%) MnO subgroups at Jalame normalised to mean values of baseline Jalame glass (samples with < 0.03 wt% MnO). Data from Table 1. Note that the three Cu- and Co–coloured samples were not included in the Mn subgroups. The punctuated line separates elements (Mo-Ni) that correlate strongly with MnO (R > 0.9) from elements that correlate less strongly (Y-As). Note log scale on y-axis. See text for details.

below 0.6 wt% (Fig. A2a), which is about the minimum that appears to have been needed to ensure effective decolourisation in a glass with 0.3% Fe$_2$O$_3$ (Silvestri et al., 2005; Zoleo et al., 2015 among others). Indeed, fourteen of the newly analysed glasses have between 0.05% and 0.25% MnO. Not only were these manganese contents ineffective for decolourisation but they cannot be considered to have regulated the colour of the glass, because the colours are very variable, including shades of olive, yellow and blue. Why did the glassmakers effectively "waste" manganese in this way and, given the value attached to colourless glass (Gliozzo, 2017), why did they not make more colourless material? The present observations suggest two possible explanations.

Firstly, the long tail of low MnO concentrations may be a reflection of inefficient batch mixing. The measured concentrations of MnO below 2 wt% are more-or-less continuous, without major compositional gaps, which suggests that specific concentrations of MnO were either not targeted or could not be achieved (Fig. A2a). Furthermore, there is evidence of inhomogeneity within single samples, for example, Ch-15 varies in MnO content from 1.7 to 2.1 wt% on a scale of centimetres (Fig. 12; referred to as Ch-15a and Ch-15b, respectively, in Table A2); it therefore seems very plausible that the variation in manganese content of a raw glass slab was substantially higher. Hence, it is inferred here that the glassmakers found it challenging to obtain a homogeneous distribution of Mn in their batch, and that melting times were insufficient to allow full homogenisation by diffusion in the molten glass. Given the presence of manganese in raw glass chunks, we assume that it was added during primary production, in which case two plausible scenarios would be: (1) it was mixed into the powdered batch before melting or (2) manganese was thrown into the furnace on top of the

molten glass. If the latter, we would expect evidence of Mn-rich aggregates which failed to be absorbed into the glass and remained at the surface; evidence of such aggregates is not apparent at Jalame, so it is assumed that the manganese ore was added to the raw materials prior to melting. If true, then several challenges had to be solved, not least the need to thoroughly mix less than one percent of MnO$_2$ with the remaining ninety-nine percent batch. Also, there are likely to have been problems of particle adhesion and segregation due to different particle sizes and densities. Such issues might have restricted the possibility of producing a glass homogeneous with respect to manganese; a slab of glass melted from a batch to which manganese had been added could therefore have shown a wide range of MnO concentrations and therefore colours. This need not have been a serious issue in practice, as the glassmakers could have sorted the glass chunks produced after the break-up of the slab by colour. Blue-green, colourless and purple chunks could have been selected for supply to glass workers, merchants or intermediaries and priced accordingly. Unfortunately the only complete glass slab for which we have several chemical analyses is that at Beth She'arim (Brill and Wosinski, 1965) which represents a failed plant ash technology and is likely of a later date than the Jalame production (Freestone and Gorin-Rosen, 1999). However, quantitative analyses of four samples from the slab show MnO contents from 0.46 to 1.08% clearly indicating difficulties in obtaining a homogeneous distribution, and consistent with the inference that this was a problem for the glassmakers of Jalame.

The second possible explanation for a low-manganese compositional tail lies in the practice of melting the primary glass batch. The glassmakers may have made batches of glass with and without high
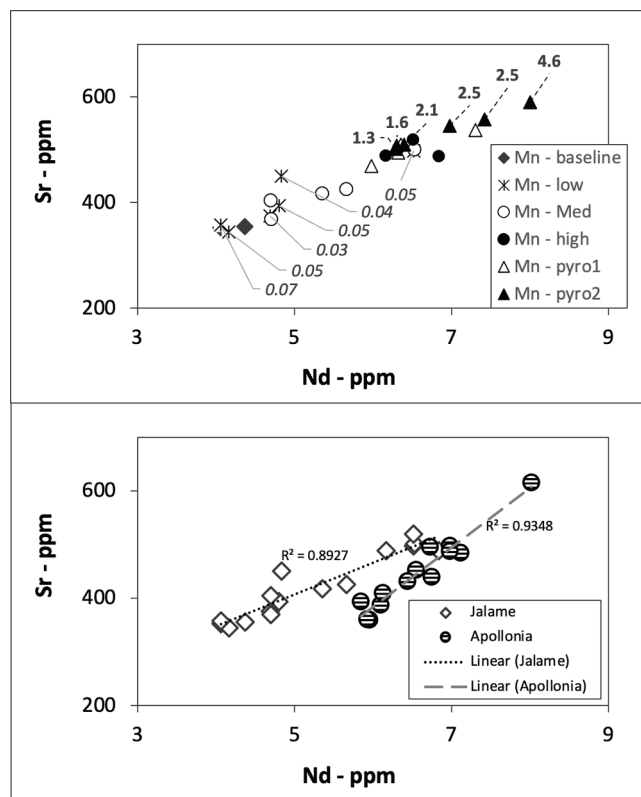
**Fig. 11.** (A). Sr [ppm] versus Nd [ppm] for all Jalame samples in this study. Mn contents [wt%] are listed next to symbols for Low Mn and Pyro-2 samples. This shows a strong correlation between Sr and Nd that is independent of Mn at levels below 1.3 wt% MnO (as illustrated by the low Mn samples), but controlled by Mn above this concentration (as illustrated by the Pyro-2 samples). (B). Sr versus Nd for Jalame samples with Mn below 1.3 wt% compared to raw glass samples from tank furnaces at Apollonia reported by Brems et al. (2018). Here, Nd and Sr correlate in glass from both glassmaking localities, but show different angles of the regression slopes. Note that three samples from Apollonia with low Sr compared to Nd (7–13 ppm) that did not fall on correlation trend were excluded from this figure.



**Fig. 12.** Analysed raw glass sample Ch-15 showing the gradual change in colour that coincides with an increase in Mn concentration. Scale in cm.

manganese. Parallels may be drawn with the ethnoarchaeological observations of Sode and Kock (2001) on primary glassmaking in India. These authors observed that large amounts of poorly fused primary glass were kept back to be remelted in later firings where they served to accelerate the melting process (Sode and Kock, op. cit. their Fig. 1 and p. 165). A situation can be envisaged where, at Jalame (and other Roman-period furnaces) poorly fused glass from previous high-manganese batches was recycled into manganese-free melts, resulting in the wide range of manganese concentrations observed.

Patterns of continuous manganese content in blue-green to colourless Roman glass very similar to those seen at Jalame are observed for example in assemblages from the UK (Jackson and Paynter, 2016) and Italy (Silvestri, 2008). At Jalame only six of twenty-five analysed weakly coloured glasses have MnO below 350 ppm, while the remainder have added manganese. This pattern is, in our view, consistent with poor mixing of manganese with the glass raw materials. Thus, the exceptionally high MnO (c. 4.6%) in one sample (Table A2: CH18) is what would be expected if mixing was problematic.

While these conclusions are somewhat speculative, the wide range of manganese contents in Levantine glass of the Roman period requires explanation, as it affects our interpretation of production processes such as recycling. We have offered two possible explanations for the phenomenon, which are not mutually exclusive, as both may have contributed to the range of MnO concentrations seen. Neither explanation is a perfect fit to the available evidence. For example, if substantial amounts of poorly melted glass were produced and recycled, why is this material not observed on the scale associated with the abandoned furnaces in India by Sode and Kock (op. cit.)? On the other hand, if there were problems in mixing small amounts of manganese into the glass batch, why is a similar phenomenon of low antimony concentrations not observed in the antimony-decolourised glass of Egypt? Roman antimony-containing glass which has no added MnO (and is therefore apparently unrecycled) rarely has $Sb_2O_5$ below 0.4% (e.g. Jackson and Paynter, 2016; Silvestri et al., 2008) implying that the mixing issues inferred for manganese decolourisation at Jalame were not encountered or were overcome. The explanation may be in the higher cost of antimony-decolourised glass (as indicated in the Price Edict of Diocletian; Stern, 1999) which was used in higher quality tablewares (Jackson and Paynter, 2021). This allowed more labour input and care to be taken in achieving a high quality product. Longer melting times, higher melting temperatures and/or a second "primary" crushing and remelting stage all seem possible, potentially implying distinct chaînes opératoires in the two regions.

### 5.3. Cobalt

The trace elements for two cobalt-blue glasses from Jalame allow for constraints on the source of cobalt used at the site. Gratuze et al. (2018) found a distinct change in the nickel that entered the glass with cobalt used during the Roman period (first-fourth centuries) and in Byzantine times (early sixth century and later). This showed the use of a low-nickel cobalt during Roman times, which yielded typical Co/Ni ratios ranging from around 24 to 54, whereas from the sixth century, this ratio decreased to between 2 and 23. The two cobalt blue glasses analysed in the present study have Co/Ni of 3.3 (Ch-14) and 10.1 (Ve-2), apparently linking the cobalt used at Jalame to the later type. Although the Jalame cobalt blue glasses contain significant MnO, due to the addition of pyrolusite or manganese oxyhydroxide phases, which would have added additional Ni to the glass, this is unlikely to have significantly affected the Co/Ni ratio. The correlation between MnO and Ni indicates that the addition of (for example) 1 wt% MnO would be responsible for only around 5 ppm extra Ni, which would not have significantly affected the Co/Ni ratios, as the Ni contents of the cobalt blue glasses are 123 and 189 ppm (Table A2).

On the basis of this admittedly small sample it is tentatively concluded that the change from low-Ni Roman cobalt to high-Ni late antique cobalt occurred around the middle of the fourth century. This is potentially significant because at about the same time, the production of Sb-decoloured glass ceased, and Sb-opacification technology was replaced by tin opacification (Tite et al., 2008). It seems possible that these marked changes in the sources of raw materials were linked and that political or economic changes in the Empire led to antimony becoming unavailable and forced the adoption of a new source of cobalt.

## 6. Conclusions

The present study demonstrates that the major element analyses published in Brill (1988) for the Jalame glasses can for most purposes be quantitatively compared with more modern data. By implication the major element analyses in the compilation by Brill (1999) may also be used. However, the earlier trace element analyses, conducted by optical emission spectroscopy, should be regarded as semi-quantitative. Indeed, Robert Brill himself showed similar caution and was clearly aware of the strengths and limitations of his data.

It has been shown that the elemental compositions of the Jalame products differ from the manganese-decolourised Roman glass found across the Roman world of the first to third centuries, particularly in terms of their higher alumina contents. While alumina is generally considered to be a potential contaminant from the melting pot or furnace, analysis of the glass–ceramic interface from the Jalame furnace materials reveals high lime and low alumina, indicating that contamination is unlikely to explain this difference in alumina concentrations. Instead, it is considered that first-third century glass was melted using sand from a different area on the eastern Mediterranean coast, probably to the North, as the glass of the primary production sites to the South of Jalame (e.g. Apollonia) are characterised by higher $Al_2O_3$ concentrations. Furthermore, in conjunction with previous results from a secondary glass working furnace, it is suggested here that alumina contamination from clay is unlikely to have been a major issue in Levantine glass production and that lime is likely to have been the major contaminant. Fourth century CE Levantine glass in Europe matches the Jalame composition and suggests that Jalame dominated production of Levantine glass at this time, although Levantine glass is frequently subordinate to Egyptian HIMT glass which appears to have been more extensively used in the West.

The opportunity to re-examine the legacy samples has been exploited to examine the extensive range of manganese contents. It is important to emphasise that Jalame is the only primary production site which has yielded an assemblage providing detailed information on the effects of manganese. Analysis by LA-ICP-MS has revealed that the addition of manganese as a colourant or decolouriser can have a major effect on some trace elements of the glass (Mo, Co, W, Zn, Ba, V, Ni) with evidence for minor contamination with a wide range of elements including lithophiles used in provenancing such as Y, Sr, the REE, Hf, Zr and Ga. Overall, effects from this latter group of elements entering the Jalame glass with Mn appear to be minor or insignificant if MnO concentrations are below 1.3 wt%.

While low concentrations of MnO, below 1.3 wt%, thus do not appear to have a major affect for these elements, caution is needed where higher MnO contents are encountered, for example in types such as Roman-Mn, Foy 2.1 and HIMT. Fortunately, these categories of natron glass are well-characterised and understood, but manganese decolourisation was also practiced widely in Islamic glass production (Henderson et al., 2016; Schibille et al., 2019) and in the production of medieval European soda-lime-silica glass (Verità, 2013) where the sources of managanese and their effects have not been investigated.

Barium and molybdenum contents suggest that two distinct sources of manganese ore (Pyro1 and Pyro2) were added to the Jalame glasses, and emphasise that the effect of manganese on the elemental composition is likely to vary with time and place. This finding, along with earlier observations on HIMT glass, suggests that it may be possible to compare the sources of manganese in other glass assemblages by using elements highly correlated with Mn, such as W and Mo.

Detailed examination of the elemental concentrations in the Jalame assemblage has also revealed strong inter-correlations inherited from the glassmaking sand, for example between Sr and Nd, the origins of which are not fully understood but which are also present in the glass from Apollonia, a primary glassmaking site where manganese was not used. Future studies on more detailed datasets and upon the sands themselves are needed to unravel these systematics, which may prove useful for better understanding natron glass source determination and production.

The wide range of manganese concentrations observed in the Jalame glass and characteristic of Mn-decoloured and weakly coloured Levantine glass of the first-fourth centuries may be explained by (a) the inability to obtain homogenous distribution of manganese ore in the batch, when the glass makers would have produced slabs showing a range of colours, which were subsequently sorted as chunks into categories such as colourless and purple glass (and possibly amber glass, where no manganese was present and the glass was reduced), to be re-melted and used to fabricate vessels, or (b) the recycling of poorly fused manganese-decolourised glass into later manganese-free batches.

The cobalt blue glasses analysed imply the introduction of late antique (high-Ni) cobalt more than a century earlier than previously inferred. This observation tentatively associates the change in cobalt source with the demise of antimony, and may suggest that the supplies of antimony and cobalt had previously been sourced in the same region or had depended upon the same trade routes.

This study has shown the value of revisiting previously studied materials using state-of-the-art techniques and carefully selecting material to address current issues. Over the past two decades there has been an explosion of glass analysis on thousands of samples. As is the case for analysed ceramics (Quinn, 2018), the archiving of scientific samples of excavated materials needs to be addressed urgently so future opportunities are not lost.

## CRediT authorship contribution statement

**Ian Freestone and Gry Barfod:** Conceptualization, Methodology, Data Interpretation, Wrote and edited drafts. **Gry Barfod:** Glass analysis, data quality. **Chen Chen:** Ceramic analysis. **Kate Larson:** Initiated project, obtained funding, curation of material, provision of samples for analysis. **Yael Gorin-Rosen:** Archaeological context. All authors: Contributed to writing, read and approved the manuscript.

## Declaration of Competing Interest

The authors declare that they have no known competing financial interests or personal relationships that could have appeared to influence the work reported in this paper.

## Data availability

all data is in the published paper

## Appendix A. Supplementary material

Supplementary data to this article can be found online at https://doi.org/10.1016/j.jasrep.2023.104179.

## References

Adlington, L.W., 2017. The Corning archaeological reference glasses: new values for 'old' compositions. Papers Inst. Archaeol. 27 (1), 1–8. https://doi.org/10.5334/pia-515.
Al-Bashaireh, K., Al-Mustafa, S., Freestone, I.C., Al-Housan, A.Q., 2016. Composition of Byzantine glasses from Umm el-Jimal, northeast Jordan: Insights into glass origins

and recycling. J. Cult. Heritage 21, 809–818. https://doi.org/10.1016/j.culher.2016.04.008.

Araffa, S.A.S., Rabeh, T.T.T., Mousa, S.E.D.A.W., Nabi, S.H.A., Al Deep, M., 2020. Integrated geophysical investigation for mapping of manganese-iron deposits at Wadi Al Sahu area, Sinai, Egypt—a case study. Arabian Journal of Geosciences 13, 1–14. https://doi.org/10.1007/s12517-020-05869-8.

Barfod, G.H., Freestone, I.C., Lichtenberger, A., Raja, R., Schwarzer, H., 2018. Geochemistry of Byzantine and Early Islamic glass from Jerash, Jordan: Typology, recycling and provenance. Geoarchaeology 33 (6), 623–640. https://doi.org/10.1002/gea.21684.

Barfod, G.H., Freestone, I.C., Lesher, C.E., Lichtenberger, A., Raja, R., 2020. 'Alexandrian' glass confirmed by hafnium isotopes. Scientific Reports 10 (1), 1–7. https://doi.org/10.1038/s41598-020-68089-w.

Barfod, G.H., Feveile, C., Sindbæk, S., 2022a. Splinters to splendours: From upcycled glass to Viking beads at Ribe. Denmark. https://doi.org/10.1007/s12520-022-01646-8.

Barfod, G.H., Freestone, I.C., Jackson-Tal, R.E., Lichtenberger, A., Raja, R., 2022b. Exotic glass types and the intensity of recycling in the northwest Quarter of Gerasa (Jerash, Jordan). J. Arch. Sci. 140, 105546 https://doi.org/10.1016/j.jas.2022.105546.

Be'eri-Shlevin, Y., Avigad, D., Gerdes, A., Zlatkin, O., 2014. Detrital zircon U-Pb–Hf systematics of Israeli coastal sands: New perspectives on the provenance of Nile sediments. J. Geol. Soc. Lond. 171, 107–116. https://doi.org/10.1144/jgs2012-151.

Bidegaray, A.I., Godet, S., Bogaerts, M., Cosyns, P., Nys, K., Terryn, H., Ceglia, A., 2019. To be purple or not to be purple? How different production parameters influence colour and redox in manganese containing glass. J. Arch. Sci. Rep. 27, 101975 https://doi.org/10.1016/j.jasrep.2019.101975.

Bouvier, A., Vervoort, J.D., Patchett, P.J., 2008. The Lu–Hf and Sm–Nd isotopic composition of CHUR: constraints from unequilibrated chondrites and implications for the bulk composition of terrestrial planets. Earth and Planetary Science Letters 273, 48–57. https://doi.org/10.1016/j.epsl.2008.06.010.

Brems, D., Freestone, I.C., Gorin-Rosen, Y., Scott, R., Devulder, V., Vanhaecke, F., Degryse, P., 2018. Characterisation of Byzantine and early Islamic primary tank furnace glass. J. Arch. Sci. Rep. 20, 722–735. https://doi.org/10.1016/j.jasrep.2018.06.014.

Brill, R.H., 1988. Scientific investigations of the Jalame glass and related finds. In: Weinberg, G.D. (Ed.), Excavations at Jalame: Site of a Glass Factory in Late Roman Palestine. University of Missouri Press, pp. 257–294.

Brill, R.H., 1999. Chemical analyses of ancient glass, volumes 1 and 2. Corning Museum of Glass, New York.

Brill, R.H., Wosinski, J.F., 1965. A huge slab of glass in the ancient necropolis of Bet She'arim. Comptes Rendus VII Internat. Cong. Glass. Bruxelles, Section B 219, 1–11.

Chen, C., Freestone, I.C., Gorin-Rosen, Y., Quinn, P.S., 2021. A glass workshop in 'Aqir, Israel and a new type of compositional contamination. J. Arch. Sci. Rep. 35, 102786 https://doi.org/10.1016/j.jasrep.2020.102786.

de Juan Ares, J., Schibille, N., Vidal, J.M., Sánchez de Prado, M.D., 2019. The Supply of Glass at Portus Ilicitanus (Alicante, Spain): A Meta-Analysis of HIMT Glasses. Archaeometry 61, 647–662. https://doi.org/10.1111/arcm.12446.

Degryse, P., 2014. Glass making in the Greco-Roman world: Results of the ARCHGLASS project. Leuven University Press. https://library.oapen.org/bitstream/handle/20.500.12657/33274/513796.pdf?sequence=1.

Emery, K.O., Neev, D., 1960. Mediterranean Beaches of Israel. Division of Fisheries, the Sea Fisheries Research Station. State of Israel, Ministry of Agriculture, Israel.

Foster, H.E., Jackson, C.M., 2009. The composition of 'naturally coloured' late Roman vessel glass from Britain and the implications for models of glass production and supply. J. Arch. Sci. 36, 189–204. https://doi.org/10.1016/j.jas.2008.08.008.

Foy, D., Picon, M., Vichy, M., Thirion-Merle, V., 2003. Caracterisation des verres de la fin de l'Antiquité en Mediterranée occidentale: L'emergence de nouveaux courants commerciaux. In: Foy, D., Nenna, M.-D. (Eds.), Echanges Et Commerce Du Verre Dans Le MonDe Antique: Actes Du Colloque De L'Association FranÇaise Pour L'Archéologie Du Verre, Aix-en-Provence Et MarseilLe, 7–9 Juin 2001. Editions Monique Mergoil, Montagnac, pp. 41–86.

Freestone, I.C., 2002. Composition and Affinities of Glass from the Furnaces on the Island Site. Tyre. J. Glass Stud. 44, 67–77. https://www.jstor.org/stable/24190872.

Freestone, I.C., Degryse, P., Lankton, J., Gratuze, B., Schneider, J., 2018. HIMT, glass composition and commodity branding in the primary glass industry. In: Rosenow, D., Phelps, M., Meek, A., Freestone, I.C. (Eds.), Things That Travelled: Glass in the First Millennium CE. UCL Press, London, pp. 159–190.

Freestone, I.C., Gutjahr, M., Kunicki-Goldfinger, J.J., MacDonald, I., Pike, A., 2015a. Composition, technology, and origin of the glass. In, Wardle, Angela (ed.) Glass Working on the Margins of Roman London: Excavations at 35 Basinghall Street, City of London, 2005. London, Museum of London Archaeology, Monograph Series, 70, pp. 75-90.

Freestone, I.C., Gorin-Rosen, Y., 1999. The great glass slab of Bet Shearim - an early Islamic glass-making experiment? J. Glass Stud. 41, 105–116. https://www.jstor.org/stable/24190848.

Freestone, I.C., Gorin-Rosen, Y., Hughes, M.J., 2000. Primary glass from Israel and the production of glass in late antiquity and the early Islamic period. MOM Éditions 33, 65–83. https://www.persee.fr/doc/mom_1274-6525_2000_act_33_1_1874.

Freestone, I.C., Jackson-Tal, R.E., Tal, O., 2008. Raw glass and the production of glass vessels at late Byzantine Apollonia-Arsuf. Israel. J. Glass Stud. 50, 67–80. https://doi.org/10.1016/j.jas.2015.07.003.

Freestone, I.C., 2021. Glass Production in the First Millennium CE: A Compositional Perspective. In: Klimscha, F. (Ed.), Ancient Glass and Glass Production. Berlin Studies of the Ancient World 67, Edition TOPOI. https://scholar.google.com/scholar_lookup?title=Glass%20production%20in%20the%20first%20millennium%20CE%

3A%20a%20compositional%20perspective&author=I.C.%20Freestone&publication_year=2021..

Freestone, I.C., Jackson-Tal, R.E., Taxel, I., Tal, O., 2015b. Glass production at an early Islamic workshop in Tel Aviv. J. Arch. Sci. 62, 45–54. https://doi.org/10.1016/j.jas.2015.07.003.

Gallo, F., Silvestri, A., Degryse, P., Ganio, M., Longinelli, A., Molin, G., 2015. Roman and late-Roman glass from north-eastern Italy: The isotopic perspective to provenance its raw materials. J. Arch. Sci. 62, 55–65. https://doi.org/10.1016/j.jas.2015.07.004.

Ganio, M., Boyen, S., Brems, D., Scott, R., Foy, D., Latruwe, K., Molin, G., Silvestri, A., Vanhaecke, F., Degryse, P., 2012. Trade routes across the Mediterranean: a Sr/Nd isotopic investigation on Roman colourless glass. Glass Technology-European Journal of Glass Science and Technology Part A 53, 217–224.

Gliozzo, E., 2017. The composition of colourless glass: a review. Archaeol. Anthrop. Sci. 9, 455–483. https://doi.org/10.1007/s12520-016-0388-y.

Gorin-Rosen, Y., 2015. Ancient Raw Glass Production in Israel: First century BCE to Eighth century CE, unpublished. University of Haifa, Haifa. PhD Thesis.

Gorin-Rosen, Y., 2000. The ancient glass industry in Israel: summary of the finds and new discoveries. In: Nenna M.-D. (Ed.) La Route du verre. Ateliers primaires et secondaires du second millénaire av. J.-C. au Moyen Âge. Lyon: Maison de l'Orient et de la Méditerranée Jean Pouilloux. MOM Éditions 33, 49-63. https://www.persee.fr/doc/mom_1274-6525_2000_act_33_1_1873.

Gorin-Rosen, Y., 2021. Wind, Sea, Sand and Fire: The Flourishing Glass Industry at the foot of the Carmel. In: As Carmel by The Sea (ed. S. Dar). Israel Exploration Society pp. 108-136. https://www.persee.fr/doc/mom_1274-6525_2000_act_33_1_1873.

Gratuze, B., Pactat, I., Schibille, N., 2018. Changes in the signature of cobalt colorants in late antique and early Islamic glass production. Minerals 8, 225. https://doi.org/10.3390/min8060225.

Henderson, J., 2002. Tradition and Experiment in First Millennium AD Glass Production The Emergence of Early Islamic Glass Technology in Late Antiquity. Accounts Chem. Res. 35, 594–602. https://doi.org/10.1021/ar0002020.

Henderson, J., Chenery, S., Kröger, J., Faber, E.W., 2016. Glass provenance along the Silk Road: The use of trace element analysis. In: Gan, F., Li, Q., Henderson, J. (Eds.) Recent Advances in the Scientific Research on Ancient Glass and Glaze, pp. 17-42.

Jackson, C.M., 2005. Making colourless glass in the Roman period. Archaeometry 47, 763–780. https://doi.org/10.1111/j.1475-4754.2005.00231.x.

Jackson, C. and Paynter, S., 2021. Friends, Romans, Puntymen, lend me your irons: The secondary glass industry in Roman Britain. In: Höpken, C., Birkenhagen, B. and Brüggler, M., (Eds.) Römische Glasöfen - Befunde, Funde und Rekonstruktionen in Synthese. Denkmalpflege im Saarland, 11 . Landesdenkmalamt Saarland, Schiffweiler, pp. 253-277.

Jackson, C.M., Paynter, S., 2016. A great big melting pot: exploring patterns of glass supply, consumption and recycling in Roman Coppergate, York. Archaeometry 58, 68–95. https://doi.org/10.1111/arcm.12158.

Kora, M., El Shahat, A., Shabana, M.A., 1994. Lithostratigraphy of the manganese-bearing Um Bogma Formation, west-central Sinai. Egypt. J. African Earth Sci. 18, 151–162. https://doi.org/10.1016/0899-5362(94)90027-2.

Kouwatli, I., Curvers, H.H., Stuart, B., Sablerolles, Y., Henderson, J., Reynolds, P., 2008. A pottery and glass production site in Beirut (BEY 015). Bulletin d'ArĆheologie et d'Architecture Libanaises 10, 103–130.

Larson, K.A., forthcoming. The Glass Blowing Waste from the 4th-century CE Workshop at Jalame, Israel. In: Annales du 22e Congrès de l'Association Internationale pour l'Histoire du Verre, Lisbon. Forthcoming.

Maltoni, S., Silvestri, A., Marcante, A., Molin, G., 2016. The transition from Roman to Late Antique glass: new insights from the Domus of Tito Macro in Aquileia (Italy). J. Arch. Sci. 73, 1–16. https://doi.org/10.1016/j.jas.2016.07.002.

Nenna, M.D., Picon, M., Vichy, M., Thirion-Merle, V., 2005. Ateliers primaires du Wadi Natrum: nouvelles découvertes. In Annales du 16e congrès de l'Association internationale pour l'histoire du verre, Londres, 2003 (pp. 56-63). Association internationale pour l'histoire du verre.

Oikonomou, A., Henderson, J., Gnade, M., Chenery, S., Zacharias, N., 2018. An archaeometric study of Hellenistic glass vessels: evidence for multiple sources. Archaeol. Anthrop. Sci. 10, 97–110. https://doi.org/10.1007/s12520-016-0336-x.

Oikonomou, A., Asscher, Y., May, H., Gorin-Rosen, Y., Rehren, T., 2023. Metal prills in primary glass: A puzzling aspect of the production process. J. Arch. Sci. Report. 49, 103977 https://doi.org/10.1016/j.jasrep.2023.103977.

Phelps, M., Freestone, I.C., Gorin-Rosen, Y., Gratuze, B., 2016. Natron glass production and supply in the late antique and early medieval Near East: The effect of the Byzantine-Islamic transition. J. Arch. Sci. 75, 57–71. https://doi.org/10.1016/j.jas.2016.08.006.

Quinn, P.S., 2018. Scientific preparations of archaeological ceramics status, value and long term future. J. Arch. Sci. 91, 43–51. https://doi.org/10.1016/j.jas.2018.01.001.

Rolland, J., 2021. Le verre de l'Europe celtique, Approches archéométriques, technologiques et sociales d'un artisanat du prestige au second âge du Fer. Sidestone Press.

Sa'id, A.A.S., Gorin-Rosen, Y., 2022. Khirbat 'Asafna. *Hadashot Arkheologiyot: Excavations and Surveys in Israel* vol. 134. https://www.hadashot-esi.org.il/Report_Detail_Eng.aspx?id=26215.

Schibille, N., Sterrett-Krause, A., Freestone, I.C., 2017. Glass groups, glass supply and recycling in late Roman Carthage. Archaeol. Anthrop. Sci. 9, 1223–1241. https://doi.org/10.1007/s12520-016-0316-1.

Schibille, N., Gratuze, B., Ollivier, E., Blondeau, É., 2019. Chronology of early Islamic glass compositions from Egypt. J. Arch. Sci. 104, 10–18. https://doi.org/10.1016/j.jas.2019.02.001.

Schreurs, J.W., Brill, R.H., 1984. Iron and sulfur related to colors in ancient glasses. Archaeometry 26 (2), 199–209. https://doi.org/10.1111/j.1475-4754.1984. tb00334.x.

Sedki, T., Mohamed, H.A., Ali, S., Zaki, R., Afeed, S., 2019. Geology and ore genesis data of Elba manganese deposits, southern Eastern Desert. Egypt. *Data in brief* 27, 104831. https://doi.org/10.1016/j.dib.2019.104831.

Silvestri, A., 2008. The coloured glass of Iulia Felix. J. Arch. Sci. 35, 1489–1501. https://doi.org/10.1016/j.jas.2007.10.014.

Silvestri, A., Molin, G., Salviulo, G., 2005. Roman and medieval glass from the Italian area: bulk characterization and relationships with production technologies. Archaeometry 47 (4), 797–816. https://doi.org/10.1111/j.1475-4754.2005.00233. x.

Silvestri, A., Molin, G., Salviulo, G., 2008. The colourless glass of Iulia Felix. J. Arch. Sci. 35, 331–341. https://doi.org/10.1016/j.jas.2007.03.010.

Slane, K.W., Magness, J., 2005. Jalame Restudied and Reinterpreted. Rei Creatariae Romanae Fautorum Acta 39, 257–261.

Sode, T., Kock, J., 2001. Traditional raw glass production in northern India: the final stage of an ancient technology. J. Glass Stud. 43, 155–169. https://www.jstor.org/stable/24190905.

Stanley, D.J., 1989. Sediment transport on the coast and shelf between the Nile Delta and Israeli margin as determined by heavy minerals. Journal of Coastal Research 20, 813–828. https://www.jstor.org/stable/4297616.

Stern, E.M., 1999. Roman glassblowing in a cultural context. American Journal of Archaeology 103, 441–484. https://doi.org/10.2307/506970.

Stevenson, K.R., Patchett, P.J., 1990. Implications for the evolution of continental crust from Hf isotope systematics of Archean detrital zircons. Geochimica et Cosmochimica Acta 54, 1683–1697. https://doi.org/10.1016/0016-7037(90)90400-F.

Tal, O., Jackson-Tal, R.E., Freestone, I.C., 2004. New evidence of the production of raw glass at late Byzantine Apollonia-Arsuf. Israel. J. Glass Stud. 46, 51–66. https://www.jstor.org/stable/24190930.

Tal, O., Jackson-Tal, R.E., Freestone, I.C., 2008. Glass from a late Byzantine secondary workshop at Ramla (South), Israel. J Glass Stud 50, 81–95. https://www.jstor.org/stable/24191321.

Tite, M., Pradell, T., Shortland, A., 2008. Discovery, production and use of tin-based opacifiers in glasses, enamels and glazes from the late iron age onwards: A reassessment. Archaeometry 50, 67–84. https://doi.org/10.1111/j.1475-4754.2007.00339.x.

Trowbridge, M.L., 1930. Philological studies in ancient glass. University of Illinois.

Verità, M., 2013. Venetian soda glass. Modern methods for analysing archaeological and historical glass 1, 515–536. https://doi.org/10.1002/9781118314234.ch24.

Vervoort, J.D., Blichert-Toft, J., 1999. Evolution of the depleted mantle: Hf isotope evidence from juvenile rocks through time. Geochimica et Cosmochimica Acta 63, 533–556. https://doi.org/10.1016/S0016-7037(98)00274-9.

Vicenzi, E.P., Eggins, S., Logan, A., Wysoczanski, R., 2002. Archeological Reference Glasses: New Additions to the Smithsonian. J. Res. Natl. Inst. Stan. 107, 719–727. https://doi.org/10.6028/jres.107.058.

Wagner, B., Nowak, A., Bulska, E., Hametner, K., Günther, D., 2012. Critical assessment of the elemental composition of Corning archeological reference glasses by LA-ICP-MS. Analytical and Bioanalytical Chemistry 402, 1667–1677. https://doi.org/10.1007/s00216-011-5597-8.

Weinberg, G.D., 1988. Excavations at Jalame: site of a glass factory in late Roman Palestine. University of Missouri Press.

Zoleo, A., Brustolon, M., Barbon, A., Silvestri, A., Molin, G., Tonietto, S., 2015. Fe (III) and Mn (II) EPR quantitation in glass fragments from the palaeo-Christian mosaic of St. Prosdocimus (Padova, NE Italy): Archaeometric and colour correlations. Journal of Cultural Heritage 16, 322–328. https://doi.org/10.1016/j.culher.2014.07.005.